# CHAPTER 145

#### EXPERIMENTAL STUDIES OF STRESSES WITHIN THE BREAKWATER ARMOR PIECE "DOLOS"

Omar J. Lillevang,\* F.ASCE and Wayne E. Nickola\*\*

## Introduction

Stresses induced within the breakwater armor piece "Dolos", when it is subjected to loads, are not reliably inferred from the twodimensional techniques of analysis used in conventional design of structures. Other methods that take the solid geometry of the dolos into consideration are available, and comprehensive application of one of them, three-dimensional photoelastic stress analysis, is reported here.

## Breakage of Dolosse

Breakage experienced at 15 projects throughout the world, where nearly 150,000 dolosse ranging from 3 to 42 short tons (2,000 pounds or 907 Kg.) in weight are in use on breakwaters, is digested for the reader by Table I. It has been impressively low. With the exception of one project, Humboldt Bay, none of those dolosse are reinforced.

It is well known that most of the breakage of pre-cast armor pieces takes place during the manufacture and storing and during the construction of the breakwater. Table I illustrates it. Several details within the table that stand out are commented upon in the following notes, each note being identified by the line number from the table:

Line 3. According to the owner's report, the relative high breakage during manufacture stems from 100°F air temperatures during casting, which contributed to development of shrinkage stresses and minute cracking.

> A wave storm during construction rolled numerous dolosse that were not yet nested in the armor matrix and they suffered impact fractures.

Breakage in service is attributed by the owner's report to battering during severe storms by loose large quarrystones.

Line 4. Most of the in-service breakage occurred when a localized area of the foundation eroded, and an abrupt subsidence into the pit caused 10 dolosse to break.

\* Consulting Engineer, Los Angeles, California \*\*Manager of Applications Engineering, Photolastic, Inc., Malvern, Pennsylvania

2519

# TABLE I

# DIGEST OF BREAKAGE OF DOLOSSE AT 15 LOCATIONS WORLDWIDE

				Short	q	er Cent Broker	
Line	Project	Year	Number	Tons	Making	Building	In Service*
1 2	Cap Aux Meules	170 170	7,418 3,934	4 6	1.0	1.0	"Limited Number"
3	Crescent City	174	246	40	2.4	6.5	2.8
4	East London	<b>'</b> 64	2,000	19.75	0.15	0.5	0.25
56 7	Gaansbaai "	170 170 170	2,786 865 928	5 13.5 18.5	<4.	0>	0.5
8	High Island	'73	6,619	27.5	"Insig."	0.8	0 ?
9	Hirtshals	י72	2,600	9.6	0.3	0.3	0.04
10 11	Honolulu	174 174	13,692 4,317	4 6	0 0	1.4 ] 1.5 ]	0.2
12	Humboldt Bay	171	4,794	42	0,02	0.02	0.75
13 14	Mossel Bay	169 169	3,423 2,634	3 6	1.0	1.2	1.0 2.0
15 16	Port Elizabeth	67 67י	14,266 13,790	3 3	4.0 ] 0.15]	"Neglig."	"Neglig."
17 18 19 20	Richards Bay	72 72 72 72 72	28,084	$\begin{bmatrix} 5.5\\ 16.5\\ 22.1\\ 33.2 \end{bmatrix}$	0.3	0.8	"Insig."
21 22	Riviere au Renard	'72 '72	7,921 1,552	5 14	3.3 2.5	0.6]-	"A Few"
23	Sandy Point	<b>'</b> 69	500	7	<b>~-</b>	1.0	>
24 25 26 27 28	Table Bay """"""""""""""""""""""""""""""""""""	169 169 171 171 174	5,900 11,700 3,000 1,500 400	3.4 6.7 3.4 6.7 11.2	0.6 0.3 <i>&lt;</i>	0.14 0.07]- 1.0	0.01
<b>2</b> 9	Thorlakshőfn	<b>'7</b> 5	2,600	9.9	0.4	1.2	1.0

\* Includes breakage during consolidation of the structures, e.g. during first storms.

2520

- Lines 5, 6, 7. Extensive litigation over the project has made factual discussion of breakage unavailable, but subsequent to consolidation of the structure it appears breakage has been nominal.
- Line 12. All but 26 of the dolosse contained steel bar reinforcement. The owner's representative reports the unreinforced versions were placed in low areas after completion of the armoring, and were thus "not integrated with other units". Of the 36 dolosse broken, 9 were not reinforced.
- Lines 13, 14. Owner's representative reports manufacturing breakage was reduced by halting cold-weather pours and changing the cementing ingredients, from 50/50 Portland cement/"slagment" to all Portland cement, during cold-weather pours.

All the dolosse were made with "all-in", pit run sandstone aggregate, resulting in concrete that was sometimes over-sanded and sometimes under-sanded. Cement was 50% Portland and 50% "Slagment", blast furnace slag.

- Line 14. In-service breakage can be separated into 1.7% initial consolidation fractures caused by insufficient fitting, and by some abrupt localized downslope adjustments, and 0.3% breakage since the consolidations during the first storms.
- Line 15. Contractor tried to use a form made of concrete for the lower half of these dolosse. Those unyielding form surfaces proved to be warped and bulged, and tended to lock in the newly cast dolosse. Excessive force was needed to remove them. When the problem was diagnosed, new fabricated steel forms were substituted and breakage immediately was all but eliminated.
- Lines 21, 22. Heavy breakage during manufacture was attributed to removal of forms when castings were only 4 hours old.
- Line 29. Contractor surmises breakage relates to steam heating of the new castings while still in the forms.

The various projects listed in Table I include many variations in materials, in quality control during manufacture, in strength of concrete and in dimensional proportions. Thus it would be surprizing if there were systematic relationships between breakage intensity and size, and there is none to be seen in the table.

Popov (4) and Danel, et al (1) have shown that armor pieces of different sizes but identically similar shape, and made of the same material, will break on impact with an unyielding surface from the same height of fall. The theory and Danel's experiments with dropping 295 tetrapods, of from 20 ounces to 25 tons weight, suggest design loads for impulsive forces on the dolos would be the same for any size piece. With other types of loads, however, steady ones or dynamic forces less severe than impacts, stresses sustained by a dolos under design conditions may be larger or smaller as the size and weight of the piece is larger or smaller. In that case there would be reason to modify the larger pieces with stress reducing measures that smaller dolosse would not require.

Three approaches toward stress management which could be combined, or be mutually exclusive, are discussed in this paper. They are:

- 1. Incorporating steel bars to take the tensile stress;
- Reduction of force moments by thickening the shank, and consequently shortening the flukes;
- 3. Reduction of stress concentrations at critical parts of the dolos by minor geometric modifications, viz. at the intersections of the flukes with the shank, to keep stresses below the modulus of rupture of the concrete.

The photoelastic tests indicate that, to have any useful effect toward preventing fracture of a dolos at its intersections of flukes with the shank, steel bar reinforcement would have to be placed so close to the skin of the piece that loss of the steel by corrosion in a short time would be unavoidable; the cost of such steel thus would be wasted and its effect would be ephemeral.

The tests suggest some stress reduction does result from thickening of the shank, but not significantly when the extent of thickening is kept below sensible limits that are proposed by the dolos' conceptor, Eric M. Merrifield. It is his view, expressed in personal communications with the senior author, that thickness of shanks in excess of 36 per cent of the height of the dolos would cause undesirable losses of interlocking characteristics.

Modifying the intersections between flukes and shank showed significant reductions of stress concentrations in the test pieces. Making dolosse of all sizes in future with a small curved fillet at those corners is proposed, not only to reduce stress concentrations but also to minimize concrete imperfections that often occur at sharp corners during pouring of concrete.

## Photoelastic Stress Analysis

Among methods of experimental stress analysis that have been developed and proved is the photoelastic study of loaded two-dimensional plastic models. Either reflection or transmission of polarized light from or through various plastic materials yields light interference patterns that are rationally related to stresses within the plastic. Knowledge of this phenomenon is not new. It has been available with use of two-dimensional models for a century, and has been in widening use since the 1930's. Beginning with discoveries made in 1936, threedimensional plastic models of complicated geometry have been loaded in

2522

laboratory ovens, at temperatures above the softening point of the model material. In this temperature range the material does soften but remains linear and deforms elastically under the applied loads. After being held under load at carefully controlled specific elevated temperatures, the oven heat is systematically and very slowly withdrawn until the model piece has reached room temperature. During this cooling phase of the "stress-freeze" process, which may take several days, the loads on the model are sustained. When the model has reached room temperature the loads can be removed, but the stress patterns persist within the plastic. The model can then be cut into thin slices at any planes of interest, and polished. When polarized light is transmitted through those slices and examined with appropriate optical equipment each one shows the stress patterns that were induced along that plane by the test loads. Calibrations and rational computation procedures relate the patterns to definitive stress values. These techniques are commonly relied upon by industry. Complicated forgings, castings, fabrications, pressure vessels, struts, bearing housings and a host of other shapes and devices have been evaluated by this method. Except for some work that may have been done in England, it apparently has not been used before on a breakwater armor piece.

#### Description of Models

Sixteen three-dimensional models of dolosse for the present tests were cast from photoelastic thermal-setting plastic. All were made with the dimension h equal to 6 inches, which is 15.24 centimeters. As will be seen in several figures in this paper, the dimension h is present in two ways in the dolos. It is the overall height from tip to tip of two adjoining flukes, and is also the overall length of the piece, measured parallel to the axis of the shank. Half the models were made with shank thickness 32 per cent of h and the other half with 35 per cent. For each thickness ratio, four different versions were cast that varied the geometric details at the intersection of the fluke with the shank. The traditional dolos, with sharp intersections between fluke planes and the planes forming the shank, was tested at both thickness ratios. Those specimens were identified by codes 32HS and 35HS, the letter S identifying the sharp intersection characteristic for pieces with shanks 32 per cent as wide and 35 per cent as wide, respectively, as the height. Other versions of corner geometry, also tested for both 32 and 35 per cent shank thickness, had chamfers created by planes (32HC and 35HC), a small-radius circular fillet (32HF and 35HF), and a larger-radius circular fillet (32H  $\phi$  and 35H  $\phi$ ).

In the stress-freeze tests, stresses frozen into the model dolosse were produced with two different loading patterns. In the "Tension" series, equal forces that were all directionally parallel with the shank's axis were applied at the ends of the four flukes. Pairs of forces were oppositely directed, in a normal sense placing the shank in tension; therefrom the "Tension" term for describing those tests. In the "Torsion" series, equal forces were again applied at the ends of the four flukes, but acting in planes perpendicular to the axis of the shank and directed to twist the shank; therefrom the "Torsion" term for that series. Sixteen models were made and stressed. Fiftyeight sections were sliced from various parallel or intersecting planes, to find the stress characteristics within the dolosse resulting with

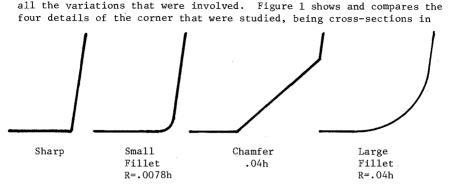


# Figure 1

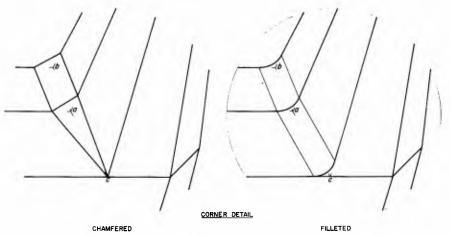
the plane common to both the fluke axis and the shank axis. As illustrated in Figure 2, the chamfer tapered to a point in the corners between planes either side of the ones cut for the profiles that are shown in Figure 1. The circular fillets in those same two flanking corners had to have radii 1.5 times as long as those in the central corner, because the angle of intersection of planes adjoining ac is larger than the angle of intersection along ab. The circular fillets did not taper to a conical point.

All the models were made with flukes whose cross-sections normal to their axes were not symmetrical octagons. The left side of Figure 3 shows the awkward geometry that develops at the intersections of flukes with the shank if a symmetrically octagonal fluke is made. To eliminate the intersection problem a slab of constant thickness, S, should be taken off the whole octagonal side of the fluke, above the shank at the intersection ab. If the maximum breadth of the octagon at the tip of the fluke is the commonly used .20h, and t is the thickness or breadth of the shank octagon, then the thickness of the slab to be removed, shown at the right side of Figure 3, is:

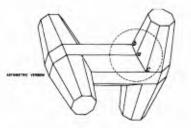
$$S = \frac{0.12132(.2t/h-t^2/h^2)}{(t/h) \operatorname{Tan} 22.5^\circ - 1} (h)$$

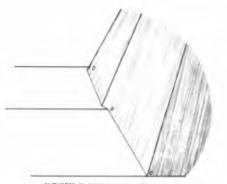
The models with chamfered and filleted corners, consistently for comparison values, also where made with flukes of asymmetrical crosssections.

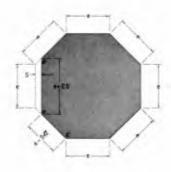
Rubber moulds for casting all the photoelastic models were formed by pouring a silicone rubber compound around a precisely machined acrylic resin master dolos that had sharp corners. To modify the master in order to make moulds for the chamfer and fillet versions, pattern maker's beeswax was hand-tooled into the corners of the master pattern. At the scale of these models, the corners of the hand-molded chamfer planes were not as sharp as one would expect intersections to be in the prototype, where structural steel plate is the likely material from which such forms would be fabricated. Because the











COMPLICATION OF FLUKE - TO - SHANK INTERSECTION WHEN CROSS-SECTION OF FLUKES IS A SYMMETRICAL OCTAGON



chamfer intersections probably were slightly rounded, the stress concentrations shown by the photoelastic models with the chamfered corners probably are less severe than they would be at prototype size, or than they would have been had the model chamfers been precisely machined instead of being hand formed of beeswax on the master pattern.

The theory of photoelastic stress analysis is well covered in reference works that are readily available in technical libraries, so there is no development of the theory in this paper. However, the laboratory techniques employed in the present tests and the analytical procedures that were followed deserve description.

A reconnaissance test program was carried out before the stress freeze models were made, to compare at least qualitatively the effects of six different arrangements of loading. For the reconnaissance, a specially compounded aluminum-filled epoxy resin was selected, and model dolosse cast from it were clad with a thoroughly bonded bi-refringent coating material. The bond was made with an epoxy-based reflective cement. A reflection polariscope was used to view the model while it was under each loading arrangement. Elastic deformations induced by the loads were transferred from the dolos to the cladding by shear forces developed at their interface. When polarized light was reflected from the surface of the model through the bonded layer, the coating exhibited patterns of birefringence which were quantitatively analyzed. Out of those preliminary tests it was concluded that the "Tension" and "Torsion" loading patterns previously described would best develop the internal stress information that was wanted from the stress-freeze photoelastic procedures.

#### Internal Stress Data, Quasi-Dimensionless Form

Stresses that were shown in the photoelastic models were reported in quasi-dimensionless form, to enable easy calculation of stresses in prototype dolosse of any size and for any selected value of the moment and shear producing forces. Stresses in the prototype were related to stresses in the model by:

$$\sigma_p/\sigma_m = (F_p/F_m) (h_m/h_p)^2$$

Where  $\sigma_{p}$ ,  $\sigma_{m}$  = Stress in prototype and model, respectively  $F_{p}$ ,  $F_{m}$  = Load on prototype and model, respectively  $h_{p}$ ,  $h_{m}$  = Corresponding dimensions of prototype and model, respectively.

If

F is expressed in units of the total dead weight p of the prototype dolos, and ρ is the unit weight of the concrete from which the prototype dolos is made, and

V is the volume of the dolos, then

$$\sigma_{\rm p}/\sigma_{\rm m} = (n \ V \ \rho/F_{\rm m}) \ (h_{\rm m}/h_{\rm p})^2$$

where n is the number of units of the dolos' weight, a convenient way to express the design load. All models were six inches high, i.e. h = 0.5 feet Thus, for models where the shank thickness t is 32 per cent of h, and Volume consequently equals .1550h<sup>3</sup>,

$$\sigma_{\rm p} = .03875 \, h_{\rm p} \, \rho \, n \, \left( \sigma_{\rm m}/F_{\rm m} \right)$$

For the models with (t/h) = 0.35 the volume is  $V = .1739h^3$ ,

So for those models it can similarly be shown that

 $\sigma_{\rm p}$  = .043475 h<sub>p</sub>  $\rho$  n ( $\sigma_{\rm m}/F_{\rm m}$ )

The test results for surface stresses then could be presented as the parameter  $\sigma/\rho h$ , and for internal stress components on the plane of each slice as  $(\sigma_1 - \sigma_2)/\rho h$ . In all cases, the numerical values of the parameter were calculated with n equal to 0.5, that is to say they are stresses induced by two forces whose sum is the dead weight of the dolos. Multiplying the numerical values of the stress parameters by the unit weight of concrete intended for a prototype dolos, in pounds per cubic foot, and the product by the height of that dolos in feet, yields stress in the prototype in pounds per stress.

#### Presentation of Results

Figures 4, 5 and 6 are examples of the forms in which stress analyses from most of the 58 slices in the complete test program were reported. Figures 4 and 5 are examples of reports on those slices that presented "Tension" test results and Figure 6 is for a "Torsion" test.

At upper right on Figures 4 and 6 the dimensions of the dolos are shown and the loading patterns of the forces F are displayed.

At top center of all sheets like Figures 4 and 6 is shown where the reported-upon slice was cut from the stress-freeze three-dimensional model.

In the photoelastic examination of each slice the optical system presented the lines of constant stress, the isochromatic fringe patterns  $(\sigma_1 - \sigma_2)$ , at full model size. It also projected the slices at ten times model size. The enlarged projections were examined to identify the locations of maximum stress concentrations at the surface and the direction of steepest gradient of stress variation within the dolos. That part of each slice was reproduced as a line drawing at the lower left of all the sheets like Figures 4 and 6, showing the surface lines of the fluke and of the shank and the intersection profile and the "contours" of the stress parameter  $(\sigma_1 - \sigma_2 / \rho h)$ . These slice displays were oriented to place the direction of the visually determined transect of steepest gradient of stresses parallel with the horizontal direction of the data sheet.

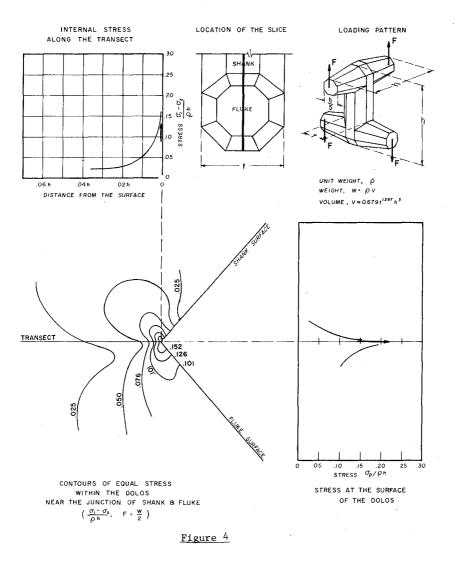
The diagram at lower right on all the sheets like Figures 4 and 6 is a direct projection, from the left, of the stress values at the surface of the dolos, and illustrate the rate of stress increase toward

SURFACE AND INTERNAL STRESS PATTERNS IN THE BREAKWATER ARMOR PIECE "DOLOS"

# SHARP CORNER; t/h=0.32

ANALYSIS OF SLICE A

TENSION TEST, NO. 32 HS1A

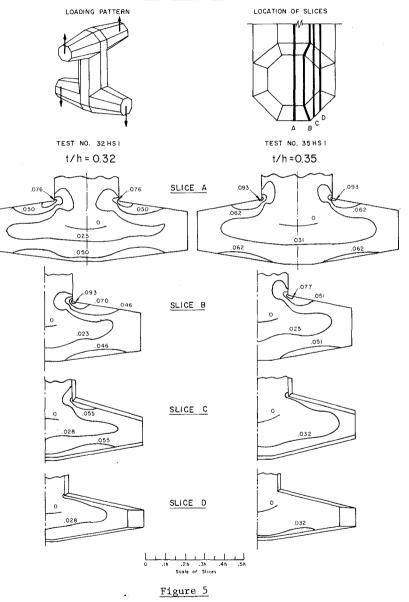


contours of internal stresses,  $\sigma_{\rm i}$  –  $\sigma_{\rm 2}$ 

IN THE BREAKWATER ARMOR PIECE "DOLOS"

"TENSION" LOADING

# SHARP CORNERS

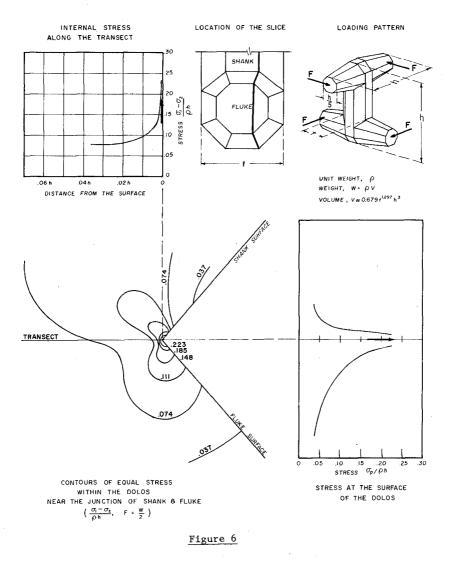


SURFACE AND INTERNAL STRESS PATTERNS IN THE BREAKWATER ARMOR PIECE "DOLOS"

SHARP CORNER; t/h=0.32

ANALYSIS OF SLICE B

TORSION TEST, NO. 32 HSB



2530

the maximum concentration at the corner. These values at the surface are the tensile stress, because  $\sigma_2$  must be zero at a free surface and the load pattern is such that  $\sigma_1$  in this case must be tensile.

At top left, the internal stress variation along the transect of steepest gradient was projected upward from the cross-section at lower left.

Stress gradients in the sharp cornered dolosse were extremely steep at the surface, and absolute determination of values at the corners was not possible. This is indicated on all plots of surface stress and of internal stress for sharp cornered pieces by small arrows, emphasizing that the value of  $\sigma/\rho h$  was not determined, and the curves stop short of joining on the Surface Stress graph and of reaching the h = 0 abscissa on the Internal Stress graph. In fact, if it were possible to make an absolutely sharp corner, the h = 0 line would be the vertical asymptote of the internal stress curve.

Four slices were taken from each "Tension" model for analysis. In models with sharp corners and with chamfered corners and with small radius filleted corners the slices were all taken at the planes described at the upper right of Figure 5. The lower parts of Figure 5 show the equal stress contours for each of the whole slices of the Tension Tests for Sharp Corners, not just the enlarged detail close to the corners that were reproduced on Figures 4 and 6. As before, numerical values for the maximum concentration of stress in the corners could not be shown, but the analysts estimated they would be on the order of 0.30 to 0.32. The rapidity with which stresses reduce, as one considers planes removed from the shank's shoulder at Slice B, is apparent when one examines the stress patterns on Figure 5 of slices C and D at successively greater offsets from the axis of the piece.

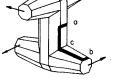
There were three slices removed from each "Torsion" test model that had sharp or chamfered or short-radius filleted corners. Two of the locations are shown at the upper right on Figure 7 and the third, a surface slab containing the corner and called Slice A, is shown on the sketch at upper left. Stress contours for all three slices are shown as before, and orthogonal trajectories of the principle stresses in Slice A are also shown. The solid orthogonals indicate the direction of the maximum tensile stress, and the dashed ones indicate the direction of the maximum compressive stress. These stress trajectories are not to be confused with the lines of constant stress, isochromatic fringe patterns ( $\sigma_1 - \sigma_2$ ), referred to as "stress contours" before in this paper. The stress trajectories represent the force flow lines of principal stress direction and are of variable stress intensity along the trajectory. Data sheets similar to Figure 7 were prepared for the Torsion tests of the chamfered and of the small radius filleted corners, but are not reproduced here.

When all data were available from testing the first three variants, with sharp, chamfered and small-radius filleted corners, comparisons were made that suggested yet another corner variation should be investigated. Table II shows maximum stress values at the surface in the corners of the three variants, all expressed as fractions of the stress STRESS TRAJECTORIES AND CONTOURS OF TORSION INDUCED INTERNAL STRESSES,  $\sigma_1-\sigma_2$  in the breakwater armor piece dolos

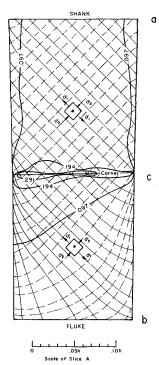
SHARP CORNER; t/h=0.32

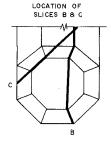
TORSION TEST NO. 32 HS



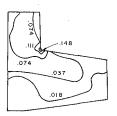


SLICE A

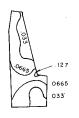




SLICE B



SLICE C



.5 h .4h .3 h Scale of Slices B & C

DEVELOPED VIEWS OF THE SLICES



analysts' best estimate of the corner concentration stresses in the sharp cornered models, which is 0.30 ph.

#### TABLE II

# RELATIVE MAGNITUDES OF SURFACE STRESS CONCENTRATIONS

	Sharp Corners	Small Fillet Corners	Chamfered Corners
t/h = 0.32 t/h = 0.32	1.00	0.73 0.80	0.63 0.63
t/h = 0.35 t/h = 0.35	1.00 1.00	0.67 0.87	0.67 0.49

Considering the analysts' view, that imprecise moulding of intersections of the chamfer planes with the fluke and shank planes tended toward understatement of stresses by the chamferred models, it appeared that the minute-radius fillet reduced stresses essentially as well as did the chamfer.

Guided by published stress reduction factors for details of common structures, a judgment was made that a dolos with circular fillets of a radius equal to 4 per cent of the dimension h should be tested. With larger radii, the published factors suggested, incremental reduction of stress concentrations became less significant. There was a concern, lest the fillet become so large that the very desirable nesting or tangling characteristic of dolosse in an armor matrix should be impaired. New stress-freeze model dolosse were made,with circular fillets of .04h radius on the corner labelled ab in Figures 2 and 3 and of 1.5 x .04h on the side corners, ac of Figures 2 and 3. As before their h dimension was 6 inches and the same Tension and Torsion loads were applied.

There were models, also as before, where the shank thickness was 32 per cent of h (t/h = .32) and where it was 35 per cent. Figures 8, 9, 10 and 11 show the results, and are directly comparable with Figures 4-7 inclusive. The pattern of slices taken from "Tension" models in these experiments was modified, as can be seen by comparing the descriptive drawing at the upper right of Figures 5 and 9. By cutting Slice C from the large fillet models on a plane radial to the fluke axis it became possible to identify the inclination and direction of the plane through the crotch of the dolos where all stress gradients were of maximum steepness. The new slice  $E_A$  was then cut along that plane. As can be seen on the slice  $E_A$  stress contour plot, at the bottom of Figure 9, the stress magnitudes are negligible along that plane. Thus, recognizing that the  $E_A$  plane is perpendicular to the A slice, and nominally coincident with the maximum gradient transect lines of the A and B slices, it is practical and conservative to use the internal stress values from slices A and B as indicative of the maximum principal stress  $\sigma_1$  (tension) rather than the principal stress difference  $\sigma_1 - \sigma_2$ .

In certain instances it is desirable to know the shear stress magnitude in concrete. This information is readily available from the

SURFACE AND INTERNAL STRESS PATTERNS IN THE BREAKWATER ARMOR PIECE "DOLOS"

# ENLARGED FILLET CORNER; t/h = 0.32

#### ANALYSIS OF SLICE A

TENSION TEST, NO. 32H0IA

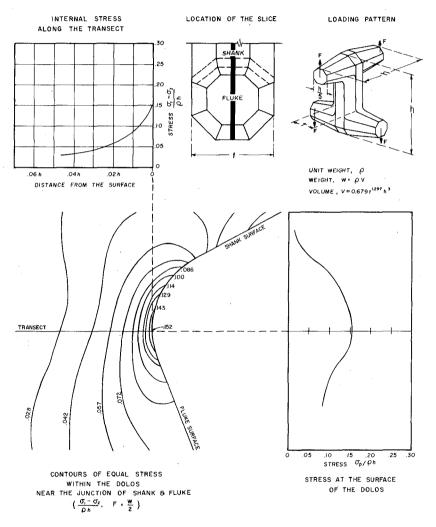
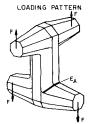
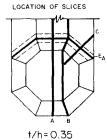


Figure 8

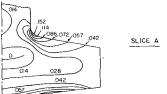
CONTOURS OF INTERNAL STRESSES,  $\sigma_1 - \sigma_2$ IN THE BREAKWATER ARMOR PIECE "DOLOS" "TENSION" LOADING

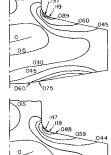
ENLARGED FILLET CORNER; t/h = 0.32 & 0.35

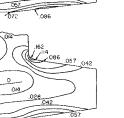


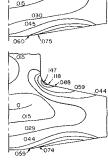


t/h=0.32











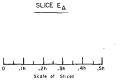
072

SLICE C

SLICE B











SURFACE AND INTERNAL STRESS PATTERNS IN THE BREAKWATER ARMOR PIECE "DOLOS"

# ENLARGED FILLET CORNER; 1/h = 0.32

#### ANALYSIS OF SLICE B

TORSION TEST, NO. 32H0B

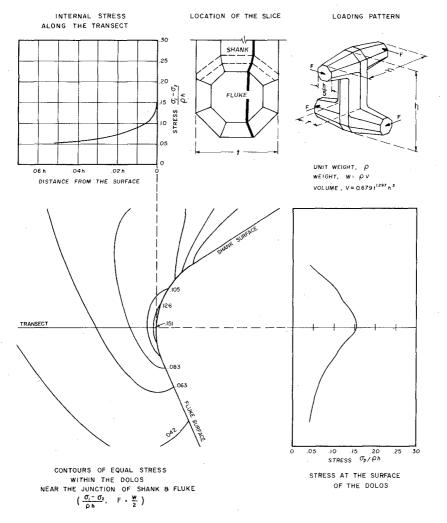
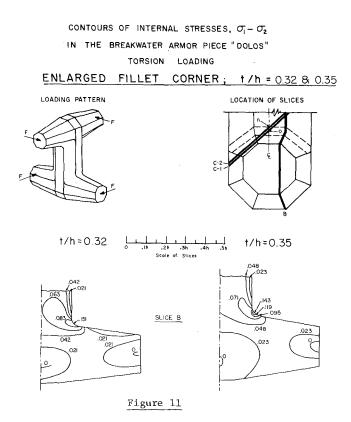


Figure 10



stress contours. The contours as shown are for the difference of principal stresses ( $\sigma_1$ - $\sigma_2$ ). From Mohr's Circle the maximum shear stress  $\tau_{max}$  is:

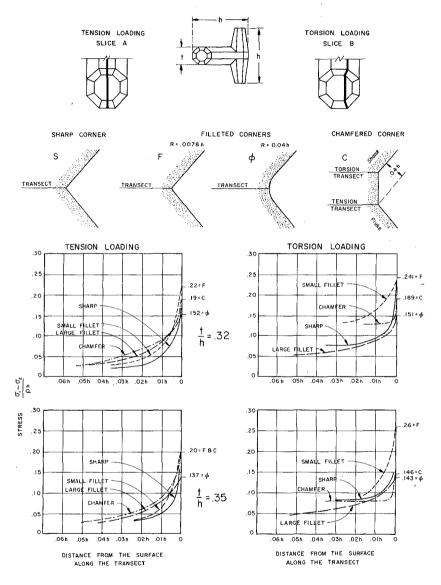
 $\tau_{max} = (\sigma_1 - \sigma_2)/2$ 

and the contours truly display 2  $\tau_{\text{max}}$  as shown.

Figures 12 and 13 each summarize and provide direct visual comparison of the internal stress gradients for all sixteen of the models that were tested. Figure 12 compares the effects of corner details and shows, to the immediate right from each graph, the numerical value of the stress parameter at the surface for each of the three corners that were not square. Recalling the analysts' estimate, that the sharp cornered dolosse had surface stress values between .30 and .32  $\rho$ h, it appears the circular fillet with radius of .04h would reduce the critical stress in the corners by 50 per cent, at least, of the sharp cornered stress value.

Figure 13 presents the same curves as Figure 12, but arranged to evaluate the effect of varying the ratio of shank thickness to dolos height, t/h.

# EFFECTS ON STRESS OF THREE FLUKE-TO-SHANK CORNER DETAILS



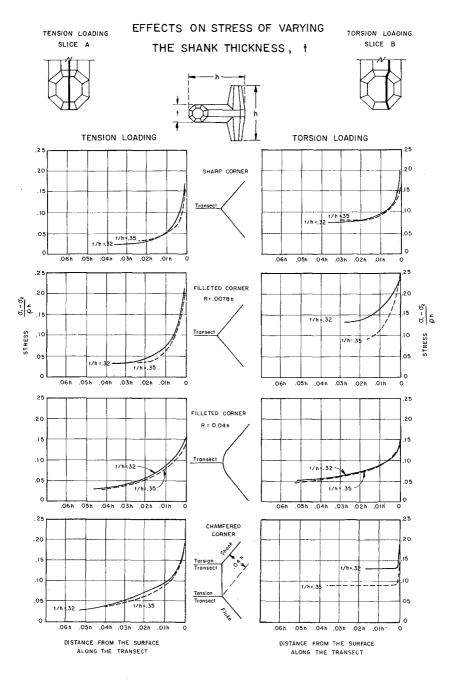


Figure 13

## Flexural Strength of Concrete

In 1957 Paul Klieger (3) presented data from comprehensive flexural tests of concretes that are remarkably systematic and are useful in considering fracture stresses in the dolos.

Beams 6 by 6 inches and supported over 18-inch spans were loaded to failure, and the tensile strengths of their concretes were calculated as the Modulus of Rupture. Strengths were determined for ages varying from one day to one year. Six-inch cubes were prepared from the ends of the broken beams and tested as compression specimens. A sufficient number of standard 6-inch diameter by 12-inch length standard cylinders also were cast from the same batches of concrete made for the beams, and they also were broken in compression. That permitted developing a reliable factor for converting cube compressive strengths to standard cylinder compressive strengths. It was determined that, for the aggregate being used, the ratio of 6" by 12" cylinder compressive strength at all ages of test specimens to the compressive strength of 6-inch modified cubes was 0.93.

One of the experimental series dealt with a concrete typical of marine structures, made with ASTM Type II cement and with air entrainment of 4.5%. One hundred forty-three test beams of ages ranging from one day to one year were tested in flexure. There is very little scatter of data from the straight line  $R = 1.1 (f_{c})^{.75}$ , where

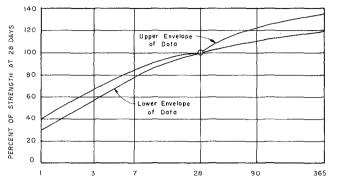
- R = Modulus of Rupture, the flexural tensile stress in pounds per square inch at the beams' extreme fibre at loads producing failure;
- $f_{c}$  = compressive strength of a standard cylinder at the age of the flexural test specimen.

Figure 14 comes from another arrangement of Klieger's data (points not plotted), to show how the Modulus of Rupture in his tests was found to vary with age of the concrete. It can be put to good practical use when making judgments as to how soon after casting a dolos one can handle it, with acceptable risks of damage to its structural integrity.

Concrete for dolosse has commonly been specified with a minimum acceptable compressive strength at 28 days of 5,000 pounds per square inch, roughly 350 Kg/cm<sup>2</sup>. The Modulus of Rupture at age 28 days for that specified compressive strength could be estimated from the Krieger experiments at 650 pounds per square inch, or  $46 \text{Kg/cm}^2$ . At one day, according to Figure 14, that same concrete might have a flexural strength of 200 pounds or more per square inch, or  $15 \text{ Kg/cm}^2$ .

A project being planned in the United States will use dolosse of the unprecedented weight of 62 short tons, which is just over 56 metric tons. If made from concrete with a specific gravity of approximately 2.4, their h dimension will be 17.5 feet, or 5.33 meters. On the same project smaller dolosse also will be placed, weighing 40 and 11 short tons. Respectively, their h dimensions would be 15.1 and 9.8 feet. Table III has been calculated from the transect curves of Figures 12 VARIATION IN MODULUS OF RUPTURE WITH TIME

TYPE II CEMENT CONCRETE WITH 4.5% AIR ENTRAINMENT FABRICATED AT VARIOUS TEMPERATURES, 73°F TO 105°F (Journal ACI, Vol.29 No.12, June 1958)



AGE OF CONCRETE, DAYS

#### Figure 14

and 13 to illustrate the stress magnitudes, under the loads F of the photoelastic experiments, at various depths in the three sizes of dolosse for the planned project.

Good practice in reinforced concrete design for hydraulic structures, particularly for a sea water environment, requires that there be substantial thickness of dense, hard, sound concrete between embedded steel and the water that surrounds or splashes the concrete. A 3-inch cover, which is 7.5 cm, commonly is required and 4 inches, nominally 10 cm, or more is required by some.

The stresses displayed in Table III suggest the reason for the low breakage experience with dolosse at existing projects that achieved uniformly high quality concrete and that were faithfully built in compliance with appropriate breakwater designs. The largest existing dolosse with sharp corners are those at East London, South Africa, and weigh just under 20 tons each. Larger ones at Hong Kong's High Island East Cofferdam (27.5 tons), Richards Bay, South Africa (33 tons), Crescent City, California (40 tons), Humboldt Bay, California (42 and 43 tons) and Sines, Portugal (44 tons) all are chamfered. Under the loading conditions used in calculating the Table III stresses, all would have surface maximum stresses of less than 650 pounds per square inch. At 4 inches depth, the closest to the surface many experienced

## TABLE III

# FLEXURAL STRESS AT THE PEAK SURFACE CONCENTRATION POINT AND $\sigma_1-\sigma_2$ AT DEPTHS, NEAR THE PEAK POINT

#### $t/h = 0.32; \rho = 150 \#/cu.ft.; F = 0.5W.$

(Pounds Per Square Inch)

Position	Corner Treatment	11 T h=9.	ons	Size & Mode of Lo 40 Tons h=15.1'		ading 62 Tons h=17.5'	
		Tension	Torsion	Tension	Torsion	Tension	Torsion
Surface Peak Stress	Sharp Sml.Fillet Chamfered Lge.Fillet	440? 325 280 235	440? 355 280 220	680? 500 430 360	680? 550 430 340	790? 580 500 420	790? 635 495 395
2" From Surface	Sharp Sml.Fillet Chamfered Lge.Fillet	50 75 115 95	125 210 195 115	105 155 205 185	215 360 300 195	140 200 250 230	255 440 350 235
4" From Surface	Sharp Sml.Fillet Chamfered Lge.Fillet	30 40 55 55	110 195 195 90	65 95 150 120	180 310 300 160	80 125 190 155	215 370 350 190

engineers want reinforcing steel placed in concrete immersed in or splashed by sea water, the stresses shown in Table III are so low that the effect of steel bar reinforcement on crack prevention might not be discernible. Such steel then would be redundant at best, because it could only act if some mortal blow striking the dolos opened a crack the bars would be incapable of preventing. For some time, the bars in such a cracked dolos might stop separation into fragments, but probably only so long as oxygenated sea water seeping to the bars through the crack had not yet completed corroding the bars to the point of severing or to exerting swelling stresses on the surrounding concrete that typically makes it spall away and create failure by that condition. It appears that reinforcing steel in dolosse must be an economic waste. However, a possibly stronger reason for not burying them within the piece is a concern such bars could induce shrinkage cracks, during hydration of cement in the freshly poured concrete.

The authors are pursuaded that large dolosse, say 30 tons and heavier, need to have eased corners between flukes and shank to reduce stress concentrations to prudent maximum levels. The use of central fillets of radius .04h and side fillets of .06h radius is seen as the best means for easing those corners, because important collateral benefits in concreting derive. Other easing geometries that are almost as effective in stress reduction do not provide as clear a concreting advantage. The relative simplicity of incorporating the fillet details when fabricating steel forms suggests it will be useful to have filleted corners in dolosse of all sizes, the concrete placing advantages being the justification.

The viewpoints expressed in the foregoing paper and conclusions reached are those of the authors. The photoelastic testing that made the paper possible were performed for Public Service Electric and Gas Company, of Newark, New Jersey. Their permission to publish the test data for the benefit of practicing engineers is acknowledged, with appreciation.

## References and Bibliography

- Danel, P., Chapus and Dhaille, "Tetrapods and Other Pre-cast Blocks for Breakwaters", ASCE Waterways and Harbors Journal, Sept. 1960.
- Hetenyi, M., "Handbook of Experimental Stress Analysis", John Wiley and Sons, Appendix II.
- Klieger, P., "Effect of Mixing and Curing Temperature on Concrete Strength", Journal American Concrete Institute, June 1958, Proceedings Vol. 54, p. 1063.
- Langhaar, H. L., "Dimensional Analysis and Theory of Models", John Wiley and Sons.
- Popov, E. P., "Introduction to Mechanics of Solids", Prentice-Hall, Inc. 1968.
- Redner, S., "Encyclopedia of Polymer Science and Technology", John Wiley and Sons, Vol. 9, pgs. 590-610.